Supporting information

Janus Group-Ⅲ Chalcogenide Monolayers and Derivative Type-Ⅱ Heterojunctions as Water Splitting Photocatalysts with Strong Visible Light Absorbance

Lei Hu[1,2], Dongshan Wei[1*]

[1] *School of Electronic Engineering, Dongguan University of Technology, Dongguan, Guangdong 523808, China*

[2] *School of Environmental and Chemical Engineering, Chongqing Three Gorges University, Chongqing 404100, China*

**To whom correspondence should be addressed. E-mail: dswei@dgut.edu.cn*

SI-1 Stability of $Ga_2X_1X_2$ (X_1, X_2=S, Se and Te) monolayers in water

To assess stability of 2D materials in water, one can calculate the enthalpy of solvation[1] or perform an electron localization function (ELF) analysis.[2] In the latter approach, the ELF value ranges from 0 to 1; ELF=1 corresponds to perfect localization of electrons (covalent bond) between the atoms; ELF=0.5 corresponds to a homogenous electron gas (metallic bond) and ELF=0 denotes complete delocalization (no bound).[3] The solubility can be further predicted from ELF analyses using bonding nature. For instance, the strong covalent bonded C_2N monolayer is insoluble in water. Obviously, ionic compounds embody good insolubility in water. The main difference of ionic and covalent compounds is the amount of charge transfer between atoms. Ionic compounds embody good insolubility in water because of large amounts of charge transfer between atoms, i.e. significant polarization of chemical bonds.

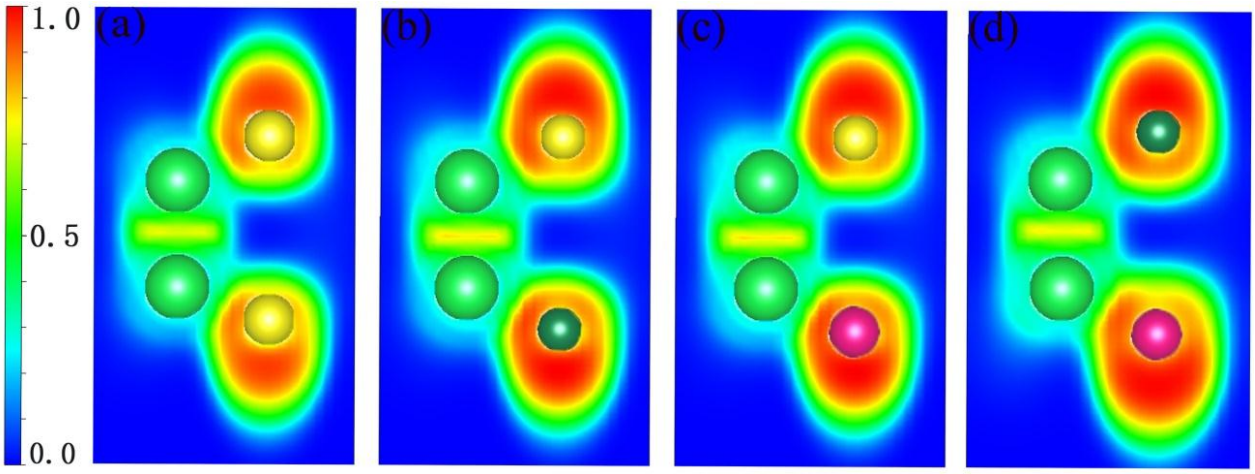

Figure S1. ELF plot along the (110) plane of (a) single-layer GaS, (b)Ga_2SSe, (c)Ga_2STe and (d) Ga_2SeTe in the unit cell.

Here, we perform ELF analyses of single-layer $Ga_2X_1X_2$. An ELF analysis of single-layer GaS is also carried out for comparison. As shown in Figure S1, ELF~1 appears around sulfur (S) atoms of single-layer GaS and $Ga_2X_1X_2$, while an ELF value of ~0.5 emerges around gallium (Ga) atoms. This suggests monolayer GaS and $Ga_2X_1X_2$ present partial ionic characters. On the other hand, the previous theoretical simulation[2] predicts single-layer WS_2 shows poor insolubility though possessing partial ionic characters, which is affirmed by the experiment where WS_2 nanosheets obtained from liquid-phase exfoliation exhibit poor insolubility in water.[2, 4] The charge transfer from the tungsten (W) atom to the sulfur (S) atom is 0.66 e in single-layer WS_2 based on Bader charge analysis. The

charge transfer from the gallium (Ga) atom to S, selenide (Se) and tellurium (Te) atoms in single-layer GaS and $Ga_2X_1X_2$ are summarized in Table S1. As can be seen, the charge transfer in single-layer GaS is comparable with that of monolayer WS_2. Another calculation suggests the GaS monolayer is stable in water,[1] which inherently implies the covalent character of S-Ga bonds. Table S1 further indicates the charge transfer between Ga and Se (Te) atoms is even reduced when compared with that between Ga and S atoms, signifying covalent characters of Ga-Se (Te) bonds. Therefore, single-layer Ga_2SSe, Ga_2STe and Ga_2SeTe are stable in water because of inherent covalent characters in the Ga-S (Se,Te) bonds.

Table S1. Charge transfer from the gallium atom to S, selenide (Se) and tellurium (Te) atoms

Materials	GaS	Ga_2SSe	Ga_2STe	Ga_2SeTe
X1	S(0.81e)	S(0.81e)	S(0.82e)	Se(0.66e)
X2	S(0.81e)	Se(0.65e)	Te(0.42e)	Te(0.43e)

SI-2 Stability of $Ga_2X_1X_2$ (X_1, X_2=S, Se and Te) monolayers and α-Ga_2S_3/Ga_2SSe heterojunctions at different strains

The structural stability under strain is very important for syntheses and applications of 2D materials. To investigate the stability at different strains, one should discuss mechanical properties.[5, 6] Thus, we calculate the stress at each strain and then plot stress-strain curves. From the turning point of stress-strain curves, we obtain the maximum tensile and compressive stresses. 2D materials will not be destroyed until the maximum stresses are exerted on.[7]

The biaxial strain effect on single-layer $Ga_2X_1X_2$ is investigated using a unit cell, as shown in Figure S2(c). Figure S2(a) suggests the maximum tensile stress of 10.92 GPa occurs at 24% strain for single-layer Ga_2SSe, namely the Ga_2SSe monolayer can sustain 24% tensile strain. Figure S2(a) further suggests Ga_2STe and Ga_2SeTe monolayers both sustain 22% biaxial tensile strain. Figure S2(b) shows single-layer Ga_2SSe, Ga_2STe and Ga_2STe respectively sustain 18%, 20% and 16% biaxial tensile strains. Similar to single-layer $Ga_2X_1X_2$, the biaxial strain effect on α-Ga_2S_3/Ga_2SSe heterojunctions is also examined on the basis of unit cells. The three Ga_2SSe/α-Ga_2S_3 heterojunctions sustain 20% biaxial tensile strain [cf. Figure S2(d)] and 16% biaxial compressive strain [cf. Figure S2(e)]. Therefore, the biaxial strains from -4% to 4% applied in the main manuscript cannot destroy

$Ga_2X_1X_2$ monolayers and $Ga_2SSe/\alpha\text{-}Ga_2S_3$ heterojunctions and can be practically realized by epitaxial growth on suitable substrate.

To check the reliability of our calculations, we reproduce of the stress-strain curve of single-layer MoS_2. As shown in Figure S2(f), the line shape in the present calculation is in agreement with that from a previous calculation.[8] The maximum stress (25.9 GPa) in the present calculation is also in good agreement with that (23.8GPa) in the previous calculation [8] and the experimental value (22$\pm$4 GPa).[9] These demonstrate that our theoretical stress-strain curves are reliable.

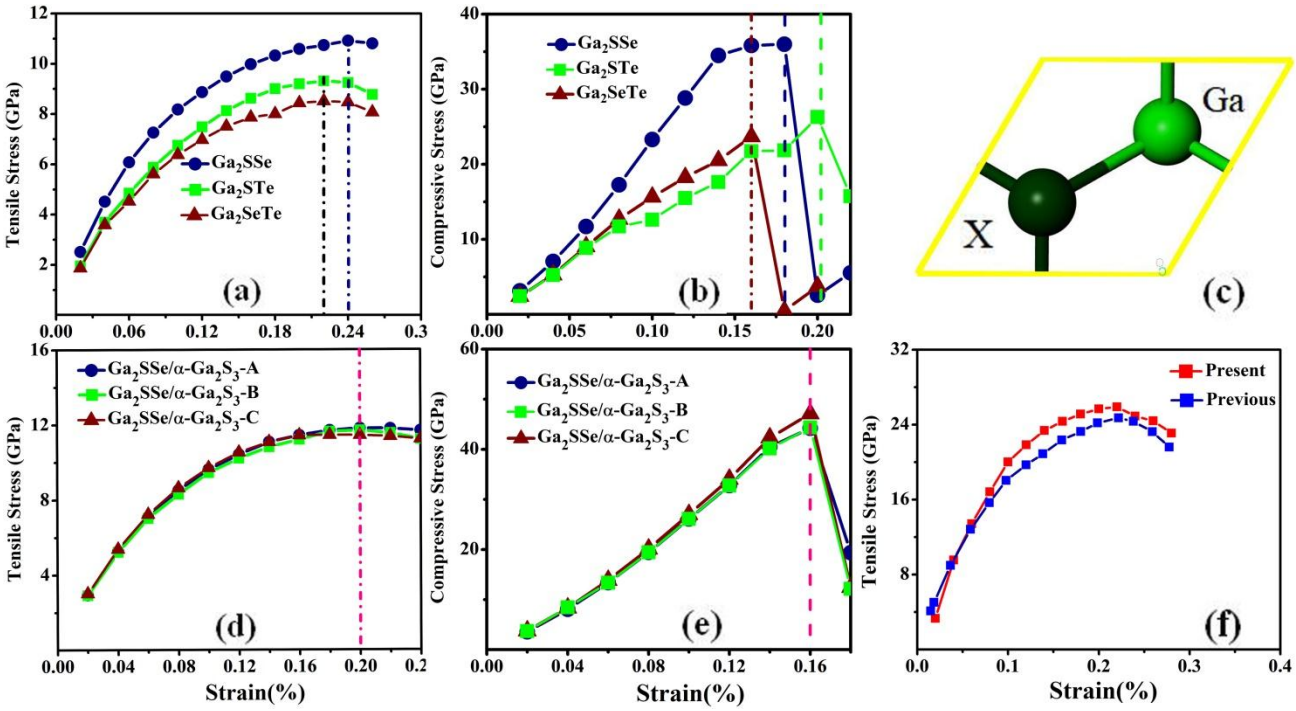

Figure S2. Stress-strain curves of $Ga_2X_1X_2$ monolayers at tensile (a) and compressive (b) strains. (c) Top view of the $Ga_2X_1X_2$ unit cell. Stress-strain curves of $Ga_2SSe/\alpha\text{-}Ga_2S_3$ heterojunctions at tensile (d) and compressive (e) strains. (f) Comparisons of the stress-strain curves of monolayer MoS_2 from different theoretical simulations.

SI-3 Formation energies and bandgaps calculated using different vdW functionals

The absorption energy and stable configuration of van der Waals heterojunctions such as $\alpha\text{-}Ga_2S_3/Ga_2SSe$ are usually connected with vdW functionals, so it's necessary to test other vdW functionals such as DFT-D3, TS, dDsC. The theoretical results are summarized in Table S2. The in-plane lattice constant and interlayer distance calculated using DFT-D3, TS and dDsC get very close to that calculated using DFT-D2. Similar to DFT-D2, the formation energies calculated with DFT-D3, TS and dDsC are negative, which further demonstrates $\alpha\text{-}Ga_2S_3/Ga_2SSe$-A,

α-Ga_2S_3/Ga_2SSe-B and α-Ga_2S_3/Ga_2SSe-C are stable 2D heterojunctions.

Table S2. In-plane lattice constant a (Å), interlayer distance d (Å), and formation energies (meV/Å^2) calculated using DFT-D2, D3, TS and dDsC

	DFT-D2			DFT-D3			DFT-TS			DFT-dDsC		
Material	a	d	E_f	a	d	E_f	a	d	E_f	a	d	E_f
α-Ga_2S_3/Ga_2SSe-A	3.617	3.806	-7.06	3.617	3.806	-7.06	3.655	3.773	-12.12	3.640	3.815	-9.06
α-Ga_2S_3/Ga_2SSe-B	3.617	3.792	-8.34	3.617	3.792	-6.97	3.664	3.726	-12.13	3.640	3.820	-8.97
α-Ga_2S_3/Ga_2SSe-C	3.620	3.066	-8.82	3.619	3.090	-11.63	3.668	3.060	-19.64	3.642	3.150	-13.31

Furthermore, we calculate the bandgaps of the Ga_2SSe monolayer and α-Ga_2S_3/Ga_2SSe-A heterojunction to test whether the electronic structures are strongly affected by the choice of vdW functional or not. As shown in Table S3, the bandgaps of Ga_2SSe and α-Ga_2S_3/Ga_2SSe-A are almost not modified with vdW functional, implying their band structures are hardly affected by vdW functional. Furthermore, optical properties are determined by electronic structure, and therefore optical properties are nearly not affected by vdW functional. Briefly, the main results about lattice parameters, electronic and optical properties will not be modified when the different vdW functional is applied.

Table S3. Bandgaps (eV) calculated using PBE-D2,PBE-D3,PBE-TS and PBE-dDsC

Material	PBE-D2	PBE-D3	PBE-TS	PBE-dDsC
Ga_2SSe	2.34	2.40	2.33	2.33
α-Ga_2S_3/Ga_2SSe-A	1.73	1.73	1.71	1.71

References

1. Zhuang, H. L.; Hennig, R. G., Single-layer group-III monochalcogenide photocatalysts for water splitting. *Chem. Mater.* **2013,** *25*, 3232-3238.

2. Kumar, R.; Das, D.; Singh, A. K., C_2N/WS_2 van der Waals type-II heterostructure as a promising water splitting photocatalyst. *J. Catal.* **2018,** *359*, 143-150.

3. Mishra, A.; Srivastava, P.; Mizuseki, H.; Lee, K. R.; Singh, A. K., Isolation of pristine MXene from Nb_4AlC_3 MAX phase: a first-principles study. *Phys. Chem. Chem. Phys.* **2016,** *18*, 11073-11080.

4. Yuan, Y.; Li, R.; Liu, Z., Establishing water-soluble layered WS_2 nanosheet as a platform for biosensing. *Anal. Chem.* **2014,** *86*, 3610-3615.

5. Garg, P.; Kumar, S.; Choudhuri, I.; Mahata, A.; Pathak, B., Hexagonal planar CdS monolayer sheet for visible light photocatalysis. *J. Phys. Chem. C* **2016,** *120*, 7052-7060.

6. Ogata, S.; Shibutani, Y., Ideal tensile strength and band gap of single-walled carbon nanotubes. *Phys. Rev. B* **2003,** *68*, 165409.

7. Nisar, J.; Jiang, X.; Pathak, B.; Zhao, J.; Kang, T. W.; Ahuja, R., Semiconducting allotrope of graphene. *Nanotechnol.* **2012,** *23*, 385704.

8. Li, T., Ideal strength and phonon instability in single-layer MoS_2. *Phys. Rev. B* **2012,** *85*, 235407.

9. Bertolazzi, S.; Brivio, J.; Kis, A., Stretching and breaking of ultrathin MoS_2. *ACS nano* **2011,** *5*, 9703-9709.